Available online at www.sciencedirect.com

ScienceDirect

Procedia Engineering 147 (2016) 366 – 371

Procedia Engineering

www.elsevier.com/locate/procedia

11th conference of the International Sports Engineering Association, ISEA 2016

Development of alpine skis using FE simulations

Fabian Wolfsperger[a]*, Denes Szabo[a] and Hansueli Rhyner[a]

[a]*WSL – Institute of Snow and Avalanche Research SLF*

Abstract

The ski manufacturing industry is characterized by short product life cycles and high innovation pressure in order to meet customer's expectations of progressive improvements of skis. To reduce development time a FE model was developed and validated to simulate the influence of changes of the ski construction on its bending and torsional stiffness. Moreover, the study aimed to evaluate the feasibility of a novel ski sandwich construction with a load dependent bending stiffness. Therefore, the FE model was used to define required strain-stiffening of a single construction layer material to reach a perceptible change of the overall ski's bending stiffness. Two existing skis with identical geometry but distinctive differences of their torsional and bending stiffness were modelled using ANSYS Workbench. The sandwich construction was modelled by 18 solid bodies with bonded contacts: core, sidewalls, edges, upper and lower face with 13 layers including 3 additional resin interlayers. Orthotropic linear elastic material properties were taken from data sheets of suppliers and from material tests of the manufacturer. Sweep meshing was used to create an all-hex mesh of solid elements. Static structural simulations of a 3-point bending test and a torsion test were run in accordance to existing laboratory tests to validate the model. For both skis, the FE model showed good agreement with the experimental data for ski A and B. The simulated overall bending stiffness (center spring constant) was, respectively 2.8% and 3.2% higher compared to the experiments. The elastic curves revealed the model as slightly too stiff at the afterbody and too soft at the forebody. The simulated torsional stiffness (torsional spring constant) was, respectively 2.1% and 4.2% lower than found in the experiments. In the development process, for example, the model was then used to quantify the influence of edge profile heights on the ski's overall bending stiffness (3% per 0.1 mm edge height). The application of strain-stiffening materials to realize a load depending ski stiffness turned as not feasible due to too small strains within the ski structure. A realistic representation of the different construction layers of an alpine ski is still challenging, especially due to the heterogeneity of the fibre compound layers and the resin distribution. Using bulk properties of the upper and lower face of the sandwich construction is not an alternative. To virtually test the influence of new materials and layups every single layer has to be represented. Using two skis for validation and additional resin interlayers for calibration appeared appropriate in order to achieve adequate model results.

© 2016 The Authors. Published by Elsevier Ltd. This is an open access article under the CC BY-NC-ND license
(http://creativecommons.org/licenses/by-nc-nd/4.0/).
Peer-review under responsibility of the organizing committee of ISEA 2016
Keywords:ski, finite elements, FEM, bending stiffness, torsional stiffness, simulation, measurement

1. Introduction

FE methods have already been used for structural and modal simulation of alpine skis as well to analyze the athlete - ski - snow interaction by implementing snow - ski boundary conditions and external forces of a skier [1 – 16]. Essential process parameters like the pressure distribution at the ski snow contact have been simulated and measured in the field in dependence on the snow properties [3 – 16]. Actual turn radii have been simulated in dependence of skier's body weight, snow hardness, edging angle and ski side cut by implementing the groove formation [7, 9, 10, 11, 15, 16]. Moreover, it was shown that numerical simulation of the ski mechanics and turns are useful to virtually test on-snow performance and deduce preliminary designs to reduce the number of on-snow tests [2, 7]. Of course, on modelling the ski- snow interaction limitations are reported such as

* Corresponding author. Tel.: +0-000-000-0000 ; fax: +0-000-000-0000.
E-mail address: author@institute.xxx

1877-7058 © 2016 The Authors. Published by Elsevier Ltd. This is an open access article under the CC BY-NC-ND license
(http://creativecommons.org/licenses/by-nc-nd/4.0/).
Peer-review under responsibility of the organizing committee of ISEA 2016
doi:10.1016/j.proeng.2016.06.314

numerically instabilities due to changing boundary conditions or the applied steady-state approach and let some authors consider the application of their model still as problematic [9]. Recently, some limitations such as over simplified snow reaction forces and the discontinuity of the ski - snow interface were overcome by Mössner et al. [16]. Nevertheless, ski - snow interaction modelling can still not be considered as state of the art in the skiing industry.

Due to increased computational power and todays user friendly FE software with CAD modules and automatic mesh generators, structural simulations of skis seemed to be more and more feasible also for smaller ski manufactures. Although highly valid methods of ski mechanics modelling were published in detail [2, 7], to the authors knowledge, the methods are not available as a commercial software application or can easily be implemented in commercial FE software. Moreover, significant deviations between the experimental and numerical results of ski mechanical parameters are stated in the literature up to 15% in bending and 20% in torsion [9]. Highly valid simulation of ski structural behavior can therefore still be considered as challenging.

We present a straightforward method to implement FE simulations into the ski development process based on standard FE software showing current limitations, possibilities and required effort. Moreover, the study aimed to evaluate the feasibility of a novel ski construction having a load dependent ski stiffness based on strain-stiffening materials. Therefore, the model was used to define the required stiffening of a single construction layer material to reach a perceptible change of the skis overall bending stiffness.

1.1. Ski model

Two existing slalom skis with identical length, width, side cut, camber and core thickness profile but different layups were modelled using ANSYS Workbench. The two skis had distinctive differences of their torsional and bending stiffness. Ski A had a high torsional stiffness and a high bending stiffness. Ski B is softer in both, torsion and bending (Tab. 2).

A CAD model of the ski geometry was built using spline functions to draw side cut and core profile which were provided by the ski manufacturer (Fig. 1b). The ski was modeled over its full core length but without shovel and tail. The sandwich construction was modelled by 18 solid bodies with bonded contacts consisting of core, sidewalls, edges, upper and lower face with 13 layers including 3 additional resin interlayers (Tab. 1).

For the ski edges a simplified L-shaped profile was used in the model with no notches (Fig. 2a). The stiffening effect of this simplification was compensated: 3-point bending simulations of short pieces (1250 mm) of both edge geometries were done. The higher bending stiffness of the simplified profile was then compensated by lowering its materials Young's modulus by a factor equal to the deflection ratio of the bending tests ($E_{compensated} = E_{steel} * 0.756$).

The layups of the two skis were provided by the ski manufacturer. By changing thicknesses and material properties of some layers one model could be used for the different skis. Ski A differs from ski B by an additional 0.5 mm bidirectional (BiD) glass fiber layer above the core. At ski B a 0.2 mm elastomer layer was inserted instead. Orthotropic linear elastic material properties were taken from data sheets of suppliers and from material tests of the ski manufacturer (Tab. 1). As the real total thickness of the skis were found 0.45 mm smaller as the sum of the layer thicknesses, three additional resin interlayers of 0.15 mm thickness were implemented. The positions of those additional resin layers influenced the ski model stiffness within a range similar to bending stiffness variations due to uncertainties of the material properties. The resin layer positions at the sandwich layup were chosen for an optimal match with the measured ski stiffness's and can be understood as a fine calibration of the model (Fig.1a).

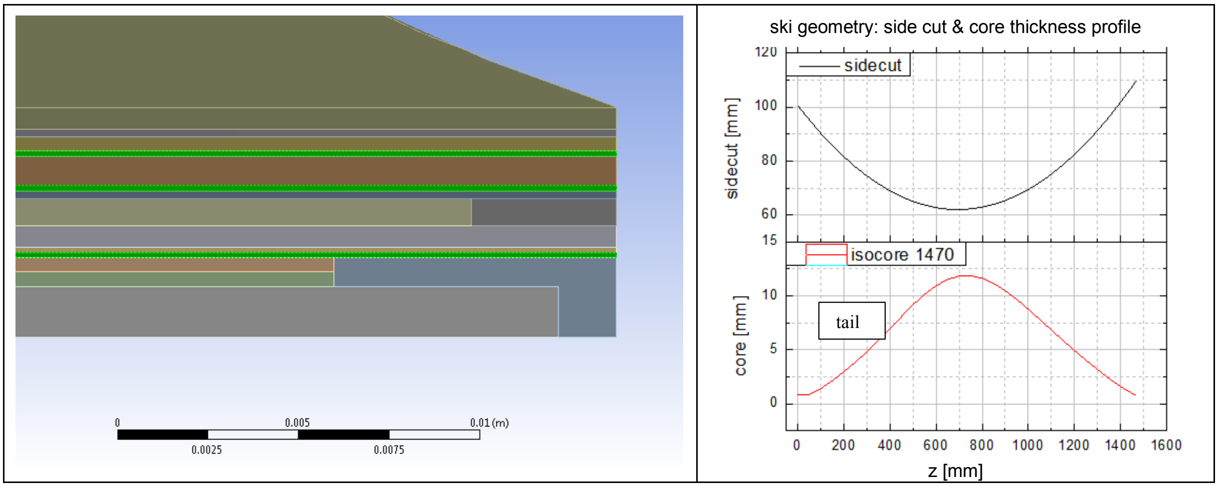

Figure 1: (a) Cross section of ski B at the tip. Additional resin layers are marked green (b) Ski geometry input data. The tail contact point is at z = 0 mm.

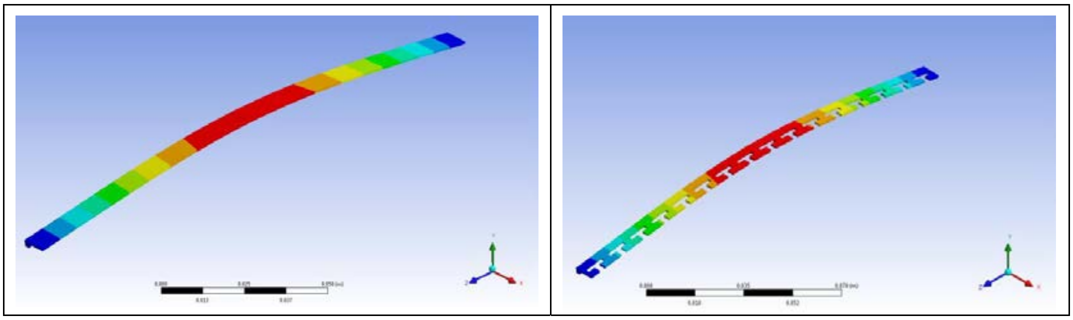

Figure 2: Three-point bending tests of edge profiles loaded with F_y = 50N showing y-deflection. (a) Simplified edge profile deflected by 18.3 mm (b) Real edge profile deflected by 24.2 mm.

Table 1: Material properties of the construction layers of ski A and B. For the glass fiber (GF) layers orthotropic material properties are given.

layer (bottom to top)	**material**	**layer thickness [mm]**	**E [GPa]**			**G [GPa]**			**poisson's ratio [-]**		
			z	**x**	**y**	**xy**	**xz**	**yz**	**xy**	**xz**	**yz**
base	polyethylene	1.1	1.2						0.4		
structural layer 1	glass fiber (UD)	0.4	32	8	8	2.5	3	3	0.32	0.18	0.18
fill up layer	phenolic resin	0.4	0.025						0.35		
edges	steel	1.9	156						0.3		
edge rubber	elastomer 1	0.13	0.0065						0.45		
interlayer 1	phenolic resin	0.15	0.025						0.35		
structural layer 2	aluminum alloy	0.6	72						0.33		
sidewalls	phenol / paper	variable	8.5						0.35		
core	polyurethane	variable	1						0.3		
structural layer 3 (ski B)	elastomer 2	0.2	0.009						0.45		
structural layer 3 (ski A)	glass fiber (BiD)	0.5	28	16	16	1	2	2	0.3	0.25	0.25
interlayer 2	phenolic resin	0.15	0.025						0.35		
structural layer 4	aluminum alloy	0.8	72						0.33		
interlayer 3	phenolic resin	0.15	0.025						0.35		
structural layer 5	glass fiber (UD)	0.4	32	8	8	2.5	3	3	0.32	0.18	0.18
fleece	polyester	0.2	2.7						0.35		
top sheet	polyamide	0.6	2						0.35		

1.2. Simulation

Sweep meshing was used to create an all-hex mesh of solid elements (solid186). Static structural simulations of a 3-point bending test and a torsion test were run in accordance to existing laboratory tests. At the 3-point bending test a fixed support was defined for the lower edge of one side of the ski and a fixed – free support was defined on the other side. A force of 329 N was applied on a 5 x 65 mm area, positioned corresponding to the laboratory tests at the boot center mark. Gravity load was also applied. The torsion test simulation used a fixed support at boot center mark. To apply a 7 Nm (ski B), respectively 13.65 Nm (ski A) torque at the shovel a rigid cylindrical body was bonded to the tip coinciding with the ski tip cross section center (Fig. 3a).

Mesh sensitivity was evaluated by comparing a 14 k versus a 27 k element mesh resulting in a change of the deflection maximum of 0.1 mm which is below the laboratory measurement uncertainty of ± 0.5 % (Tab. 2). A 14 k mesh was therefore considered as sufficient.

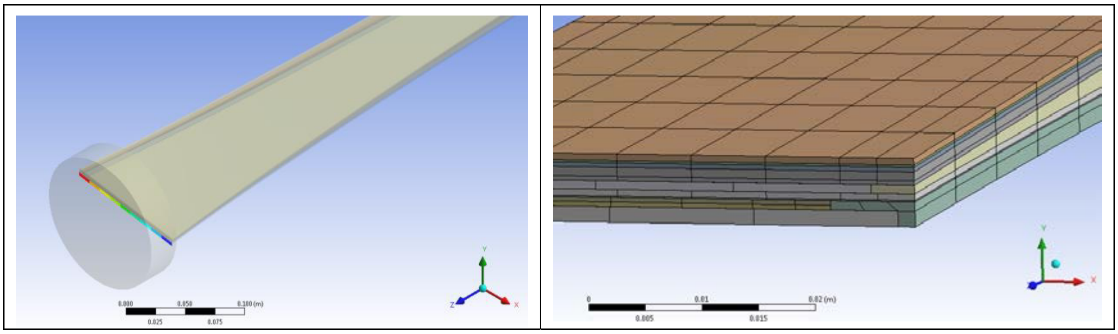

Figure 3: (a) Simulated torsion test of ski A. A body bonded to the tip was used to apply the torque. (b) Ski model: 14 k all-hex mesh was used for the simulation.

1.3. Laboratory Tests

At the 3-point bending test setup the skis were supported at the beginning and the end of the skis' core which were also coincident with tip and tail contact points (Fig. 4a). The skis were loaded up to a force of 329 N which was continuously recorded using a miniature ring load cell (type 8438 – 6001; Burster Präzisionsmesstechnik GmbH & Co. KG, Gernsbach, D). The deflection curve of the loaded ski was measured in 4 mm steps along the ski with an automatically moving laser displacement transducer (Type CP35MHT80; Wenglor Sensoric GmbH; Tettnang, D). The center spring constant b (also called overall bending stiffness or flex) was then derived by the maximum deflection and the applied load. A torsion test was conducted for the forebody of the ski (Fig. 4b). The ski was rigidly fixed at the boot center mark while an increasing torque was applied at the shovel until a torsion angle of 8° was reached, which is a realistic torsional ski deformation during skiing [12]. Torsion angle and torque was continuously recorded by a rotary potentiometer and a miniature ring load cell. The torsional spring constant t (also called torsional stiffness or twist) of the ski forebody was then derived by the maximum torsion angle and the applied moment.

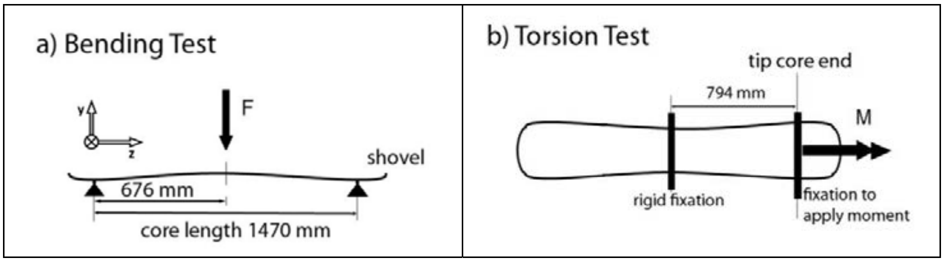

Figure 4: (a) Setup 3-point bending test. (b) Torsion test.

2. Results

2.1. Model validation

For both skis, the FE model showed good agreement with the experimental data for ski A and B. The simulated center spring constants were slightly lower compared to the measurements. The elastic curves revealed the model as slightly too stiff at the afterbody and too soft at the forebody (Fig. 5). The simulated torsional spring constants were slightly higher than found in the experiments. The relative error of the simulated tests was within ± 5 % for each of the four loading / layup cases (Tab. 2).

The inserted elastomer layer above the core of ski B, which was replacing the 0.5 mm glass fiber layer of ski A, resulted in a decrease of 13.9 % of the center spring constant. The torsional spring constant dropped even more by 48.3 % due to the highly elastic elastomer layer (Tab. 2).

Table 2: Model validation data: Comparison of measured (meas) and simulated (sim) bending and torsional spring constants of ski A and B.

mechanical property	**parameter_ski**	**measurement** (n=3) mean ± s	**simulation**	**Δ relative [-] (meas – sim) / mea**
torsional spring constant	t_A [Nm/°]	1.705 ± 0.013	1.740	-0.021
	t_B [Nm/°]	0.882 ± 0.004	0.918	-0.041
Δ relative	(t_A – t_B) / t_A [-]	0.483	0.472	
center spring constant	b_A [N/mm]	5.101 ± 0.011	4.939	0.032
	b_B [N/mm]	4.391 ± 0.006	4.270	0.028
Δ relative	(t_A – t_B) / t_A [-]	0.139	0.157	

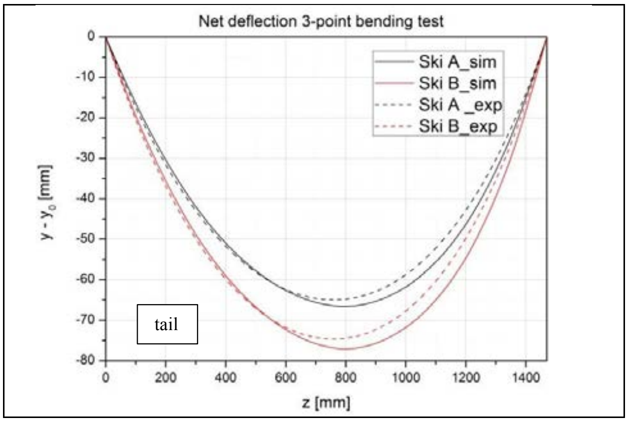

Figure 5: Measured and simulated net deflection curves of ski A and ski B. The ski's tail contact point is coincident with z = 0 mm.

Table 3: Maximum ski deflection at 3-point bending test

max. deflection / camber [mm]	measurement	simulation
ski A	65.0 / 9.1	66.7 / 3.7
ski B	74.6 / 5.6	77.1 / 3.7

2.2. Model applications

The validated model provides an in depth information on the stresses and strains in different layers in dependence of the specific loading case (Fig. 6). During bending major loads are taken by the aluminum and glass fiber layers of the lower face of the sandwich construction. Identified the load bearing structures, the stress or strain components and distributions are of interest. For example, to find an optimal position for embedded damping inlays for the first torsion mode the skis strain energy maximum was located (Fig. 7a). Furthermore, the simulations were used as virtual prototype testing to quantify the influence of layer thicknesses or new materials on the ski's stiffness. For example, the impact on the center spring constant of new steel edges with larger profile heights (2.2 vs. 1.9 mm) was quantified: An increase of the center spring constant of 3% per 0.1 mm edge height was found.

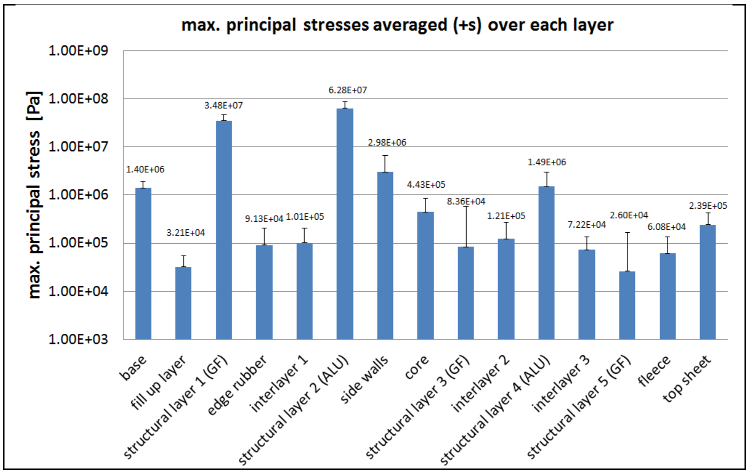

Figure 6: Maximal principal (±s) stresses averaged over each construction layer of ski A.

Recent advances were reported in realizing strain stiffening behavior in synthetic polymers networks at relatively low values of strain [18]. Normal strains in the lower face layers were found only up to 0.15 % which is far to less to reach strain stiffening effects. During bending shear strains were found distinctively higher up to 15 %, but only locally at tip and tail of the bended ski structure (Fig. 7b). Simulations with hypothetical material properties for the fill up resin layer showed that a desired strain-stiffening material would need to exhibit an increase from 1 to 63 GPa of its elastic modulus. By that, a load dependent increase of the center spring constant of 10% would be realized, which was shown as perceptible even for recreational skiers [19].

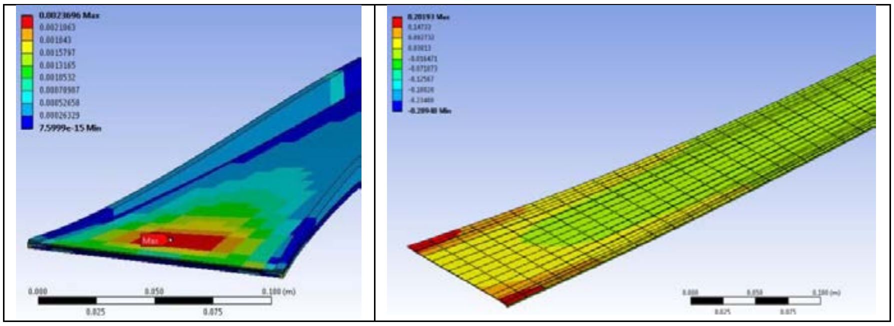

Figure 7: (a) Global strain energy maximum [J] at the lower aluminum layer during torsion at ski A. (b) Shear strains [m/m] in the edge rubber layer at ski tip.

3. Discussion

The generated FE ski model with implemented boundary conditions for a virtual bending and torsion test showed good agreements with the experimental data. Due to unavoidable uncertainties of the material properties, especially of resin and glass fiber layers, deviations of a few percent between measurements and simulation have to be considered as a realistic representation of the manufacturing tolerance of the skis. Based on the high validity of the model, FE simulation could be applied to define the requirements for the application of strain-stiffening materials and virtually test the influence of changes of thickness, stiffness and position of the different construction layers. Moreover, a deeper general understanding of the structural behavior of the ski construction could be gained.

4. Conclusion

A realistic representation of the different construction layers of an alpine ski is still challenging, especially due to the heterogeneity of the fiber compound layers and the resin distribution. Using bulk properties of the upper and lower face of the sandwich construction is not an alternative. To virtually test the influence of new materials and layups every single layer has to be represented. Using two skis for validation and additional resin interlayers for fine calibration appeared appropriate in order to achieve adequate model results. The described applications enhanced both efficiency and innovation of the development process. Further steps are to implement additional boundary condition setups to bring the virtual mechanical testing closer realistic on-piste loading situations.

References

[1] Piziali RL, Mote CD Jr. (1972). Snow ski as a dynamic system. ASME J Dyn Syst Meas Control Ser G 94: 133–138.
[2] Nordt, A. A., Springer, G. S. and Kollár, L. P. (1999). Computing the mechanical properties of alpine skis. Sports Eng 2 (2): 65–84.
[3] Renshaw AA, Mote CD Jr (1989). A model for the turning snow ski. Int J Mech Sci 31: 721–736.
[4] Casolo F., Lorenzi, V., Vallatta, A., Zappa B. (1997). Simulation techniques applied to skiing mechanics. In: Müller E, Schwameder H, Kornexl E, Raschner (eds) Science and skiing. Taylor & Francis, pp 116–130.
[5] Hirano Y., Tada N. (1996). Numerical simulation of a turning alpine ski during recreational skiing. Med Sci Sports Exerc 28:1209–1213.
[6] Tada N, Hirano Y (1999). Simulation of a turning ski using ice cutting data. Sports Eng 2 (1): 55–64.
[7] Nordt A. A, Springer GS, Kollar LP (1999). Simulation of a turn on alpine skis. Sports Eng 2 (3):181–199.
[8] Kaps P, Mössner M, Nachbauer W, Stenberg R (2000). Pressure distribution under a ski during carved turns. In: Proceedings of the 2nd international congress on skiing and science, pp 180–202.
[9] Federolf P., Roos M., Lüthi A. (2010). Finite Element Simulation of the Ski-Snow Interaction in a Carved Turn in Alpine Skiing. Sports Eng 12 (3): 123-133.
[10] Federolf P., Lüthi A., Roos M., Dual J. (2010). Parameter Study using a Finite Element Simulation of a Carving Alpine Ski to Investigate the Turn Radius and its Dependence on Edging Angle, Load, and Snow Properties. Sports Eng 12 (3): 135 – 14.
[11] Brennan, S.M., Kollar, L., Springer, S.(2003).Modelling the mechanical characteristics and on-snow performance of snowboards. Sports Eng 6 (4): 193-206.
[12] Scott, N., Yoneyama, T., Kagawa, H., Osada, K. (2007). Measurement of ski snow-pressure profiles. Sports Eng10 (3): 145-156
[13] Yoneyamaa, T., Kitadea, M. Osadab, K. (2010). Investigation on the ski-snow interaction in a carved turn based on the actual measurement. The Engineering of Sport 8. pp. 2901–2906
[14] Brown CA (2009). Modeling edge-snow interactions using machining theory. In: Müller E, Lindinger S, Stoggl T (eds). Science and skiing 4. Meyer & Meyer Sport (UK) Ltd., pp 175–183.
[15] Mössner M, Heinrich D, Schindelwig K, Kaps P, Lugner P, Schmiedmayer H, Schretter H, Nachbauer W (2006). Modeling of the ski–snow contact for a carved turn. In: Moritz EF, Haake S (eds) The engineering of sport 6. Springer, New York, pp 195–200.
[16] Mössner M, Heinrich D, Schindelwig K, Kaps P, Schretter H, Nachbauer W. (2014). Modeling the ski-snow contact in skiing turns using a hypoplastic vs an elastic force-penetration relation. Scand J Med Sci Sports 24(3).
[17] Vogel, S. (2011). FBG - deformation measurement of skis during riding. Feasibility study for a measurement system with fiber Bragg gratings. Master Thesis. Institut des Matériaux, Swiss Federal Institute of Technology Lausanne. Ref. Prof . Dr Veronique Michaud, F. Wolfsperger (SLF).
[18] Erk K, Henderson KJ, Shull KR. (2010). Strain stiffening in synthetic and biopolymer networks. Biomacromolecules 11(5):1358-63.
[19] Fischer, C., Fauve, M., Combaz, E., Bourban, P.E., Michaud, V., Plummer, J.G., Rhyner, H.U., Manson, J.A. (2006). What static and dynamic slalom skis should possess: judgments by advanced and experts skiers. Journal of Sports Science 25: 1567-1576.